Vol. 549: 183–198, 2016
doi: 10.3354/meps11706

MARINE ECOLOGY PROGRESS SERIES
Mar Ecol Prog Ser

Published May 10

Modeling the migration of the American eel in the Gulf of St. Lawrence

Mélanie Béguer-Pon[1,2,*], Kyoko Ohashi[2], Jinyu Sheng[2], Martin Castonguay[3], Julian J. Dodson[1]

[1]Département de Biologie, Université Laval, Québec City, Québec G1V 0A6, Canada
[2]Department of Oceanography, Dalhousie University, Halifax, Nova Scotia B3H 4R2, Canada
[3]Institut Maurice-Lamontagne/Fisheries and Oceans Canada, CP 1000, Mont-Joli, Québec G5H 3Z4, Canada

ABSTRACT: Telemetry experiments allow documentation of aquatic animal movements in the ocean, and numerical models can contribute to our understanding of the mechanisms underlying the observed movement patterns. In this study, we used mature (silver-stage) American eel *Anguilla rostrata* migration out of the St. Lawrence Estuary (SLE)–Gulf of St. Lawrence (GSL) system to illustrate how an individual-based model coupled with a 3-dimensional ocean circulation model can help us understand fish behaviour, and complement ongoing and future telemetry experiments. A suite of 23 numerical simulations that combined various vertical and horizontal swimming behaviours of virtual eels ('v-eels') was conducted to evaluate which behaviours most closely matched the observed migratory patterns of silver eels in the GSL. Results indicated that v-eels migrating through the SLE–GSL must employ active swimming and complex orientation strategies in order to migrate in the time suggested by telemetry experiments. The use of selective tidal stream transport is sufficient for v-eels to escape entrapment in the Estuary; however, this behaviour requires active swimming rather than simply drifting in the direction of the appropriate currents in the Estuary in order to eventually exit the GSL within the time frame observed in the field. Orientation towards higher salinity and/or greater water depths in the Gulf was not sufficient for v-eels to successfully escape the GSL, suggesting the use of other variables such as the geomagnetic field gradient is required. The model also allows exploration of the potential effects of climate change on the duration of migration, through changes in hydrological conditions.

KEY WORDS: Orientation cues · Telemetry · Particle-tracking · Spawning migration · Ocean Tracking Network · Ocean circulation model · *Anguilla rostrata*

INTRODUCTION

Recent advances in aquatic telemetry have revolutionized our capabilities for observing animals in the ocean and for acquiring detailed information on movements of free-ranging aquatic animals in space and time (Hussey et al. 2015). Theoretical methods such as mechanistic models can help us understand the underlying mechanisms of the observed movement patterns (Bauer & Klaassen 2013). Individual-based models (IBMs, also called agent-based models) have increasingly been used to simulate movements of aquatic animals (Tang & Bennett 2010, Bauer & Klaassen 2013). The most frequently-used approach for assessing routes, schedules, and behaviour during the migration of marine animals is to incorporate a physical transport model as a sub-model within the IBM (Bauer & Klaassen 2013). This approach has been used to test various direction-finding mechanisms of salmon during their homeward migration (Thomson et al. 1992, 1994, Healey et al. 2000, Putman 2015). Such modeling approaches have also been used to study the migration of the larvae of anguillid eels (e.g. Kettle & Haines 2006, Bonhom-

*Corresponding author: melanie.beguer@gmail.com

meau et al. 2009, Rypina et al. 2014). Recently, the long-distance migration of the American eel *Anguilla rostrata* and European eel *A. anguilla* was simulated from their respective continental shelves to their spawning areas in the Sargasso Sea to explore the role of the physical marine environment and test hypotheses about the eels' orientation and navigation mechanisms (Béguer-Pon et al. 2016).

Silver-stage American eels leaving the fresh waters of the St. Lawrence River (SLR) (Canada) must travel down the St. Lawrence Estuary (SLE) and across the Gulf of St. Lawrence (GSL) before reaching the open ocean and continuing toward the Sargasso Sea. Migration across the GSL represents a minimum swimming distance of about 800 km in a semi-enclosed sea of 226 000 km^2. The GSL has an estuarine-type circulation driven partly by freshwater discharge from the SLR (Koutitonsky & Bugden 1991). Since 2010, several animal-tracking experiments have been conducted as part of the Ocean Tracking Network, resulting in the first documentations of the migratory patterns of silver eels from the upper SLR to the south end of the Gulf (Béguer-Pon et al. 2012, 2014). The use of selective tidal stream transport (STST) — in which out-migrating silver eels occupy surface waters on the outgoing tide to maximize downstream transport but remain close to the bottom on incoming tides to reduce upstream transport — has been supported by observations in the SLE (Béguer-Pon et al. 2014); however, evidence for such behaviour appears equivocal in other areas (Parker & McCleave 1997, Bradford et al. 2009). In the GSL, silver eels perform diel vertical migrations (DVM) (Béguer-Pon et al. 2012), as has been observed for several anguillid species worldwide during their marine migrations (e.g. Aarestrup et al. 2009, Schabetsberger et al. 2013, Chow et al. 2015). In the GSL, a migration route in the deep Laurentian Channel has also been supported by observations (Béguer-Pon et al. 2012). Satellite tracking experiments conducted on the Scotian Shelf have suggested that thermohaline gradients and fronts could act as orientation cues in the early phase of the eels' marine migration (Béguer-Pon et al. 2015). While the horizontal temperature gradient in the upper water column of the GSL during October–December is weak, and thus an unlikely horizontal orientation cue, the near-surface salinity increases from the SLE (about 28) to the south end of the GSL at Cabot Strait (about 32) and thus could guide migrating eels out of the Gulf. The bathymetry could also act as an orientation cue to exit the GSL, assuming that eels are able to sense it. Recent studies have argued that fish are able to determine their depth using a mechanism that involves changes in swim-bladder volume and vertical speed (Taylor et al. 2010, Holbrook & de Perera 2011). Eels could also use the geomagnetic field to either navigate or orientate toward their final destination (Durif et al. 2013, Putman et al. 2014). The geomagnetic field intensity decreases from the northwestern part of the GSL to its southeastern part, and therefore this gradient could help eels in orientating toward Cabot Strait. Béguer-Pon et al. (2015) also hypothesized that eels could use a combination of magnetic intensity and inclination angle to assess their geographic locations and truly navigate (using a bi-dimensional map), as has been shown for juvenile Pacific salmon (Putman et al. 2014).

Understanding the extent to which different environmental variables influence the migration of American eels, and therefore their success in exiting the GSL, is crucial, particularly given the precarious status of the species in Canada and especially in the upper SLR and Lake Ontario (COSEWIC 2012). Maturing eels leaving the SLR–Lake Ontario system are almost exclusively females, and are also the largest eels found in the entire distributional range of the species. They are therefore the most fecund of American eels (Castonguay et al. 1994, Tremblay 2009, Jessop 2010) and likely represent a major contribution to the reproductive potential of this panmictic species (Côté et al. 2013).

In the present study, we coupled an individual-based model with a 3-dimensional ocean circulation model to simulate the migration of silver-stage American eels from the SLE to the southern exit of the GSL at Cabot Strait. Our main objective was to evaluate which swimming behaviours (vertical or horizontal) allowed virtual eels (hereafter 'v-eels') to reproduce the migration pattern, timing, and trajectories observed by telemetry experiments recently conducted in the SLE and GSL (Béguer-Pon et al. 2014, Castonguay et al. 2015). We first tested the hypothesis that STST with active swimming in the direction of the ebb tide (as opposed to drifting) would be a sufficient behaviour to allow eels to escape estuarine circulation and entrapment. Secondly, we tested 2 alternative hypotheses concerning migration out of the GSL: (1) that reference to simple environmental gradients of salinity and water depths would be sufficient to explain the observed migratory performance of eels while traversing the GSL; and (2) that successful migration requires highly orientated swimming behaviour beyond that provided by simple environmental gradients. The potential effect of extreme river discharge values on the timing of migration of v-eels was also examined.

MATERIALS AND METHODS

The Gulf of St. Lawrence and ocean circulation model

The SLE–GSL system (Fig. 1) is one of the largest semi-enclosed seas in the world by surface area (ca. 226 000 km^2). Its main source of fresh water is the SLR. Downstream of Québec City, fresh water from the SLR meets the upstream extent of saltwater intrusion at the head of the SLE. About 450 km downstream of Québec City, the Estuary connects with the GSL. Exchanges between the GSL and the North Atlantic Ocean occur mainly through Cabot Strait in the southeast GSL, which has a width of ~100 km. A smaller amount of exchange also occurs through the Strait of Belle Isle in the northeast GSL. A major bathymetric feature of the GSL is a deep trough, the Laurentian Channel, which begins at the continental slope outside of the GSL and extends landward through Cabot Strait into the GSL, with one channel shoaling in the SLE and 2 channels shoaling in the northeast GSL. The Laurentian Channel reaches a maximum water depth of 540 m. The southwest portion of the GSL, known as the Magdalen Shallows, has water depths of generally less than 80 m (Koutitonsky & Bugden 1991).

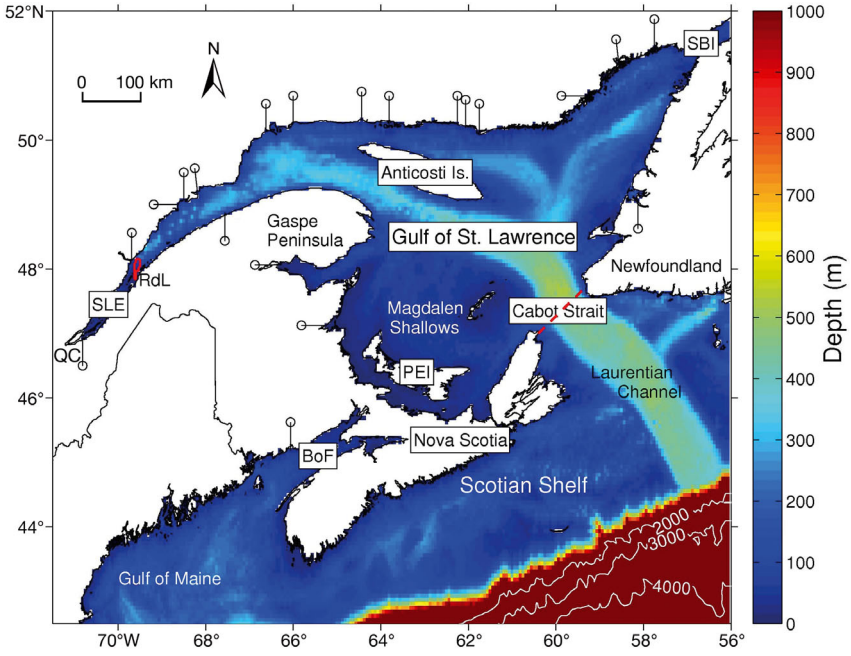

Fig. 1. Study area (and a portion of the circulation model domain) and its major bathymetric features for the virtual eel (v-eel) simulation. RdL: Rivière-du-Loup; SLE: St. Lawrence Estuary; SBI: Strait of Belle Isle; PEI: Prince Edward Island; BoF: Bay of Fundy, QC: Quebec City. Black lines with open circles: idealized channels that represent rivers in the model; solid red line in the SLE: initial release area of particles. The red dashed line accross Cabot Strait denotes the exit of the Gulf of St. Lawrence; v-eels that move offshore (southeast) of this line are considered to have exited the Gulf

Fig. 2 shows the monthly-mean fields of salinity and currents at 5 and 100 m depths in November 2011, simulated by the ocean circulation model used in this study (described below). Circulation in the SLE is characterized by a surface-intensified outward (nearly eastward) flow driven mainly by freshwater discharge from the SLR. Outflow from the SLE continues eastward along the coast of the Gaspé Peninsula as the Gaspé Current. This current leaves the coast at the eastern tip of the Peninsula and continues southeastward, eventually exiting the GSL through Cabot Strait (mainly on its western side). The general circulation pattern in the GSL is also characterized by northeastward flow along the New-

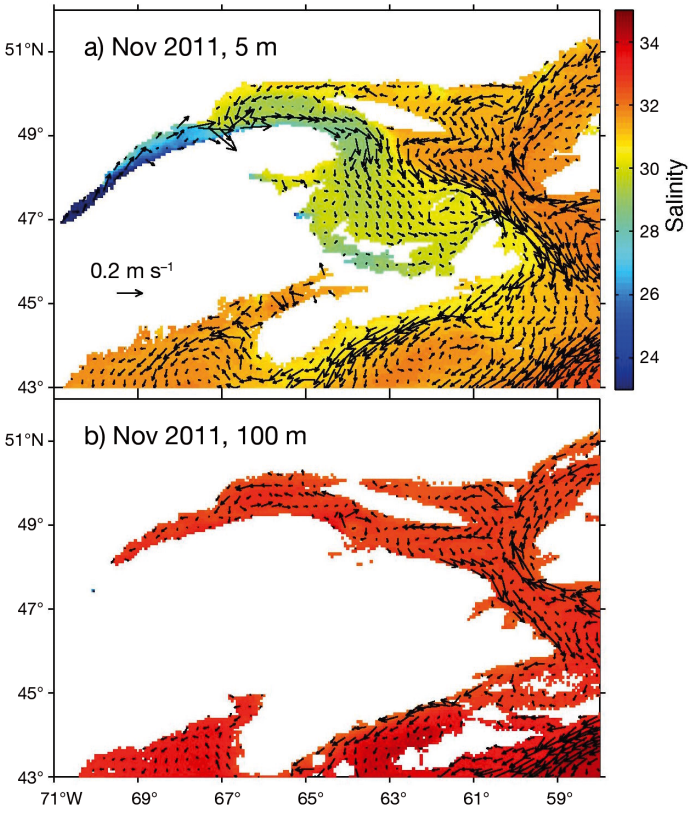

Fig. 2. Monthly-mean fields of salinity and currents for November 2011 calculated from model results at depths of (a) 5 m and (b) 100 m over the St. Lawrence Estuary, Gulf of St. Lawrence, and eastern Scotian Shelf. Velocity vectors are shown at every fourth grid point

foundland coast and westward flow along the north shore; the latter combines with a recirculating branch of the Gaspé Current to form a cyclonic gyre (the Anticosti Gyre) over the northwest GSL. The near-surface salinity field (Fig. 2a) has a distinct spatial pattern, with the low values (<29) occurring in the SLE, and a salinity front running diagonally across the GSL that separates an area of lower (<31) salinity to its southwest and higher (>31) salinity to its northeast. The subsurface salinity field (Fig. 2b) is more homogeneous horizontally (ca. 32 to 34) than the surface field. The circulation and salinity fields during the remainder of the 120 d study period (data not shown) have similar horizontal features to those in November, except that the near-surface salinity just north of the SLE increases from ca. 30 to 31.

Ohashi & Sheng (2013, 2015) developed a 3D circulation model capable of reproducing the major features of the regional circulation and hydrography; the model is based on the Princeton Ocean Model (Mellor 2004). The model domain covers an area from 38.5° to 52° N, and from 71.5° to 56° W, which includes the GSL, the Scotian Shelf, and the Bay of Fundy–Gulf of Maine system. The horizontal resolution of the model is 1/16° in both the longitudinal and latitudinal directions. The model uses the terrain-following sigma-coordinate system, with 40 sigma layers in the vertical. A description of the model set-up is given in the Appendix. The 3D fields of hourly currents and salinity are used to drive the IBM.

The numerical particle-tracking model

An individual-based numerical model with 3D fields of circulation and hydrography was developed for this area and is described in detail in Ohashi & Sheng (2015). The particle-tracking model in the present study incorporates the directed swimming motion (horizontal and vertical) that was published in Ohashi & Sheng (2015) along with new programmed behaviours not previously published. The hourly displacement of each v-eel is calculated as the vector sum of displacement due to the horizontal swimming behaviour and the displacement due to the current at the eel's position:

$$\frac{d\vec{x}}{dt} = \vec{u}_P(\vec{x},t) + \vec{u}_B(\vec{x},t) \quad (1)$$

where $\vec{x}$ is the position of the v-eel at time t, $\vec{u}_P(\vec{x},t)$ is the velocity of the water with respect to the geographic frame of reference, and $\vec{u}_B(\vec{x},t)$ is the velocity of the eel as it swims through the water.

Simulated eel swimming behaviours

Vertical behaviours. Two swimming behaviours that allowed v-eels (i.e. particles with active behaviour) to move vertically were specified in the IBM: STST and DVM. Virtual eels that exhibited STST moved near the bottom (20 m above the bottom for waters deeper than 60 m, or 90% of the water depth for shallower waters) and remained stationary if the ambient ocean current had a landward component, regardless of the time of day. If the ambient current had a seaward component or a value of zero, the v-eels swam (active STST) or drifted (passive STST) in the direction of the ocean current (either at any time or only during the night, depending on the simulation), and moved near the surface (20 m from the surface) at night and remained near the bottom during the day. V-eels were allowed to use STST in the Estuary and in the Gulf until the near-surface salinity was >30 (near-surface salinity is generally <30 within the SLE, the area to the north of the Gaspé Peninsula, and over the Magdalen Shallows). Previous observations from satellite and acoustic tagging experiments have suggested that silver eels do not use STST as they pass through Cabot Strait, with tagged eels being recorded at the acoustic array during various tidal periods (Béguer-Pon et al. 2012, 2014). A salinity value of 30 was used in this study for v-eels to stop performing STST in the Gulf.

DVM was previously observed for silver eels equipped with pop-up archival satellite tags while migrating through the GSL (Béguer-Pon et al. 2012). In the GSL, eels fitted with satellite tags reached a maximum depth of 370 m during the day (Béguer-Pon et al. 2012). Observations made in the open ocean, however, indicated that silver eels can swim much deeper, to a depth of 1200 m (Aarestrup et al. 2009, Béguer-Pon et al. 2015, Wysujack et al. 2015). Thus, it appears likely that eels can reach the bottom while in the GSL (ca 500 m). V-eels that perform DVM were programmed to move instantaneously to the near-bottom (i.e. 20 m above the bottom for waters deeper than 60 m, and 90% of the water depth for shallower waters, as mentioned above) at sunrise and to the near-surface (20 m from the surface) at sunset. Previous observations demonstrated that eels ascend to the surface or descend to the bottom within 1 h, indicating that it is reasonable, as a first-order of approximation, to consider that v-eels undertake DVM instantaneously in the numerical simulations presented in this paper. V-eels were set to undertake DVM during the whole tracking period. As previously described, STST incorporates DVM. In

simulations where STST and DVM were not in effect, particles were free to move vertically; the vertical displacements were due to both vertical currents and very small random vertical movements that mimiced small-scale mixing. Detailed numerical expressions of the vertical and horizontal behaviours used in this study are provided in Ohashi & Sheng (2015).

Horizontal behaviours. A total of 5 horizontal swimming behaviours were considered: (1) randomly chosen compass bearings, (2) navigation (programmed adjusted bearing) or compass orientation toward the exit of the Gulf, (3) orientation toward greater depth, (4) orientation toward higher salinity, and (5) orientation toward both greater depth and higher salinity. In the case of random movement, v-eels were programmed to swim in a direction randomly selected from among all possible directions at each time step. In the case of navigation/compass orientation, 2 cases were considered depending on the use of STST in the Estuary. In the first case, v-eels did not use STST in the Estuary but were set to constantly swim (24 h d^{-1}) toward a point just outside the SLE (50° N, 65.75° W) until reaching an area north of the Gaspé Peninsula (to exit the Estuary) and then modify their swimming behaviour to swim toward a point within Cabot Strait (46.75° N, 59° W). The v-eels generally swam northeastward during the first part of the trip and southeastward during the second part, but the exact direction depended on their position relative to the point towards which they were swimming. In the second case, v-eels used STST in the Estuary, and once the salinity reached 30 they were set to swim in a different direction each hour, with the probability that the swimming direction would be in a general southeastward direction (in the 90° range between southward and eastward) increased to 0.5 (from 0.25 in the case of randomly chosen swimming directions). The southeastward swimming preference could be explained by the decreasing gradient of geomagnetic field intensity that exists from the northwest to the southeast in the GSL, as previously mentioned. The northeastward swimming preference cannot be explained by the geomagnetic gradient but could be a complex combination of environmental factors acting together (salinity, odour, water depth and temperature).

In the case of orientation towards higher salinity or greater water depths, each v-eel was set to check the salinity or water depth in the 8 model grid boxes surrounding the grid box in which it was located. If a v-eel did not find higher salinity or deeper water among the surrounding model grid points, it would swim in a random direction. Numerical simulations conducted by Ohashi & Sheng (2015) demonstrated that distributions of particles are sensitive to the frequency at which v-eels check their surrounding conditions, and that performing the search too frequently would cause the v-eels to become 'trapped' in local features. Based on these results, v-eels with a preference for higher salinity were set in this study to search for higher salinity every 4 h during the night (when they were near the surface), and those with a preference for greater water depths were set to search for deeper waters every 2 h during the day (when they were near the bottom).

Numerical simulations

We conducted a suite of 23 numerical simulations that combined the previously described behaviours (Table 1). In each simulation, v-eels were released at 00:00 h UTC on 28 October 2011 over an area near Rivière-du-Loup, Québec in the SLE (Fig. 1) and tracked with a time step of 1 h for 120 d. The time and release locations were chosen to match those of the acoustic tracking experiment conducted in the SLE–GSL system (Béguer-Pon et al. 2014). V-eels were initially placed 100 m apart horizontally in an area spanning 47.625° to 48.375° N, and 69.625° to 69.500° W, resulting in 11 921 v-eels released in each simulation. To test the robustness of the results with respect to the number of v-eels used, the simulation that involved active STST, DVM and a preference for southeastward swimming (simulation DB) was repeated with different initial distances between the v-eels: 20 m (298 216 v-eels), 50 m (47 677 v-eels), 200 m (2963 v-eels), and 500 m (490 v-eels). There were no significant differences among these simulations. Since simulations with drifting particles (passive, no active swimming movements) released from the same area showed that most particles are still trapped in the Estuary after 60 d (Ohashi & Sheng 2015), only simulations with active behaviours were examined in this study. V-eels were programmed to start moving at the beginning of the first ebb tide following release (10 h after release). In all simulations, the individual horizontal swimming speed was fixed at 0.5 m s^{-1} in order to compare the performance of the various behaviours. To assess the effect of the individual horizontal swimming speed, 5 additional values were examined in simulations DB and OD (see Table 1 for simulation descriptions): 0.2, 0.8, 1.0, 1.2, and 1.5 m s^{-1}. These speed values were used in swim tunnel experiments using male and female European eels, and the optimal speed at 18°C was estimated to be be-

Table 1. Numerical simulations (N = 23) of virtual eel (v-eel) behaviour conducted with different combinations of parameters. Note that all simulations except DB were conducted using the St. Lawrence River (SLR) discharge of 2011. Sws: swimming speed of v-eels; STST: selective tidal stream transport; DVM: diel vertical migration

Simulation name	Vertical behaviours	Horizontal behaviours	Sws ($m\ s^{-1}$)	Year of SLR discharge value	N
R	None	Random direction	0.5	2011	1
RS	Active STST	Random direction	0.5	2011	1
RSD	Active STST + DVM	Random direction	0.5	2011	1
RSDN	Active STST + DVM	Random direction	0.5[a]	2011	1
DBW	DVM	Orientation toward NE while in the Estuary and then toward Cabot Strait	0.5	2011	1
DB	Active STST + DVM	Orientation toward Cabot Strait	0.2, 0.5, 0.8, 1.0, 1.2, 1.5	2011, dry year, wet year and 1955–2014 average[b]	9
DBP	Passive STST + DVM	Orientation toward Cabot Strait	0.5[c]	2011	1
OD	Active STST + DVM	Orientation toward deeper depths	0.2, 0.5, 0.8, 1.0, 1.2, 1.5	2011	6
OS	Active STST + DVM	Orientation toward higher salinity	0.5	2011	1
OSD	Active STST + DVM	Orientation toward both higher salinity and deeper depth	0.5	2011	1

[a]V-eels swam only at night during STST (in contrast to the other simulations, in which during STST they swam whenever seaward currents occurred)
[b]Scenarios with dry, wet and 1955–2014 average discharge values were run only for sws = 0.5 $m\ s^{-1}$
[c]Sws = 0 in the case of passive STST in the Estuary

tween 0.7 and 1.0 body lengths (BL) s^{-1} (van den Thillart & van Ginneken 2007, Burgerhout et al. 2013a,b). All simulations were initially conducted using the SLR discharge of 2011. To assess the potential impact of higher or lower discharge on the migration of v-eels, 3 additional sets of SLR discharge values were studied using simulation DB: a 'dry' year, a 'wet' year, and a climatological annual cycle (the mean for the period between 1955 and 2014). Wet and dry years were calculated by first determining the maximum and minimum discharge values between 1955 and 2014 (max. of 25 752 $m^3\ s^{-1}$ in May 1974; min. of 7822 $m^3\ s^{-1}$ in Sep 1964); the May mean discharge +3 SD and the September mean discharge −3 SD gave values similar to the maximum and minimum values of the records. The discharges of wet and dry years represent the results of respectively adding and subtracting 3 SDs from the climatological values.

Model outputs and comparison of numerical simulations

For each simulation, the cumulative proportion of v-eels that reached Cabot Strait (Fig. 1) was calculated at each time step of the model and plotted for visual comparison of the relative successes among different simulations. Maps showing the distribution of all v-eels after 28 d of tracking were drawn, as well as trajectories during 120 d of 10 randomly chosen v-eels (the same 10 v-eels were used for all simulations). To compare the distribution of v-eels after 28 d of particle tracking, the centre of mass of v-eels was calculated (the average longitudinal and latitudinal coordinates of all v-eels). The averages and SDs of the spread of v-eels about their centres of mass were also used in the analysis. The distribution of successful v-eels at Cabot Strait was computed by calculating the distance from the southern end of Cabot Strait for each v-eel that crossed the Strait.

To put the outputs from the *in silico* simulations into perspective with the observations, the observed range of migration durations was superimposed onto plots representing the percentage of v-eels that reached Cabot Strait versus time. The observed range of migration durations was obtained from acoustic tracking experiments conducted in the Gulf between 2011 and 2013 (Béguer-Pon et al. 2014, authors' unpubl. data). Since 2011, a 125 km acoustic receiver line has allowed monitoring of the presence of

tagged fish at the southern end of the Gulf at Cabot Strait (Fig. 1) (Castonguay et al. 2015). In total, 34 silver eels were detected at Cabot Strait within a period of 12.8 to 67.2 d after their release in the SLE; half of which were detected between 20 and 37 d of release. The number of eels detected at Cabot Strait was a small proportion of the eels that were tagged and released in the SLE (over 300 eels; authors' unpubl. data). Béguer-Pon et al. (2014) argued that this low detection rate could have been due to various factors, including a 2-step migration process (i.e. some eels could have stopped their migration in the Gulf and resumed it the following season). This would not have been detected due to the battery life of the acoustic tags (between 147 and 195 d). Assuming some of the eels had stopped their migration and resumed it later, the migration duration would be greater than that based on observed detections. In this paper, we therefore considered the observed range of migration duration as being that of the most active eels, and our objective was to evaluate which behaviours would allow us to reproduce the migration timing of only those eels.

In the case of simulations aimed at evaluating the potential effect of low and high SLR discharge values, differences in the duration of v-eels' migration between simulations were statistically assessed using Student's *t*-test.

RESULTS

Success escaping the Gulf of St. Lawrence

Half of all numerical simulations designed to compare the effects of different behaviours resulted in some success (Table 2). Success in this study was defined as the proportion of v-eels that reached the southern end of the Gulf at Cabot Strait within 67 d (the longest observed migration duration). Among the successful simulations, DBW — in which v-eels were programmed to constantly swim toward the Estuary exit and then toward Cabot Strait — was most successful, with 100% of v-eels reaching Cabot Strait within 20 d.

Inclusion of STST behaviour allowed the v-eels to escape entrapment caused by the estuarine circulation in the Estuary; swimming with appropriate tidal currents (i.e. active STST) instead of drifting with appropriate currents (passive STST) was required in order to escape the Estuary in less than 2 wk. In simulation R (in which v-eels swam in a random direction), v-eels remained trapped in the Estuary for the entire tracking period (120 d). By comparison, most v-eels in simulations RS and RSD (in which STST was performed) escaped the Estuary and were halfway to Cabot Strait approximately 28 d after release (Fig. $3b_2$,c_2). Simulation RSDN, in which v-eels moved only at night while performing STST in the Estuary, showed a lower efficiency than RSD, in which v-eels moved regardless of the time of day (success at 67 d was reduced by 41.5%; Table 2). The efficiency of the active (as opposed to passive) STST behaviour can be analysed based on major differences between simulations DB and DBP. In these 2 simulations, v-eels all performed STST, but in DBP they did not swim actively during the appropriate tidal currents. As a result, v-eels in DBP had a longer migration duration in the Estuary (43 d to reach 67.125° W) and a null

Table 2. Numerical simulations of virtual eel (v-eel) behaviour conducted with different combinations of parameters. Sws: v-eel swimming speed; SLR: St. Lawrence River; CBS: Cabot Strait acoustic line

Simulation	Sws ($m\ s^{-1}$)	Year of SLR discharge value	% of v-eels reaching the CBS after 67 d	Migration duration (d)	
				Fastest v-eel	Slowest v-eel
R	0.5	2011	0	>120	>120
RS	0.5	2011	33.5	45.4	>120
RSD	0.5	2011	49.3	49.4	>120
RSDN	0.5[a]	2011	28.8	55.2	>120
DBW	0.5	2011	100	19.6	20.6
DB	0.5	2011	100	34.2	48.6
DB	0.5	Dry	86.1	36	69.3
DB	0.5	Wet	100	33.2	46.2
DB	0.5	1955–2014 average	100	34	50.2
DB	0.2	2011	84	53.9	79
DB	0.8	2011	100	23.3	37.4
DB	1	2011	100	20	33.6
DB	1.2	2011	100	16.6	34.2
DB	1.5	2011	100	13.7	33.9
DBP	0.5	2011	0	82.9	>120
OD	0.2	2011	20.2	62.3	94.2
OD	0.5	2011	71.7	49.6	>120
OD	0.8	2011	48.8	41.2	>120
OD	1	2011	41.4	38.2	>120
OD	1.2	2011	36.3	36	>120
OD	1.5	2011	31	31.9	>120
OS	0.5	2011	0	>120	>120
OSD	0.5	2011	0	>120	>120

[a]V-eels swam only at night during STST (in contrast to the other simulations, in which during STST they swam whenever seaward currents occurred)

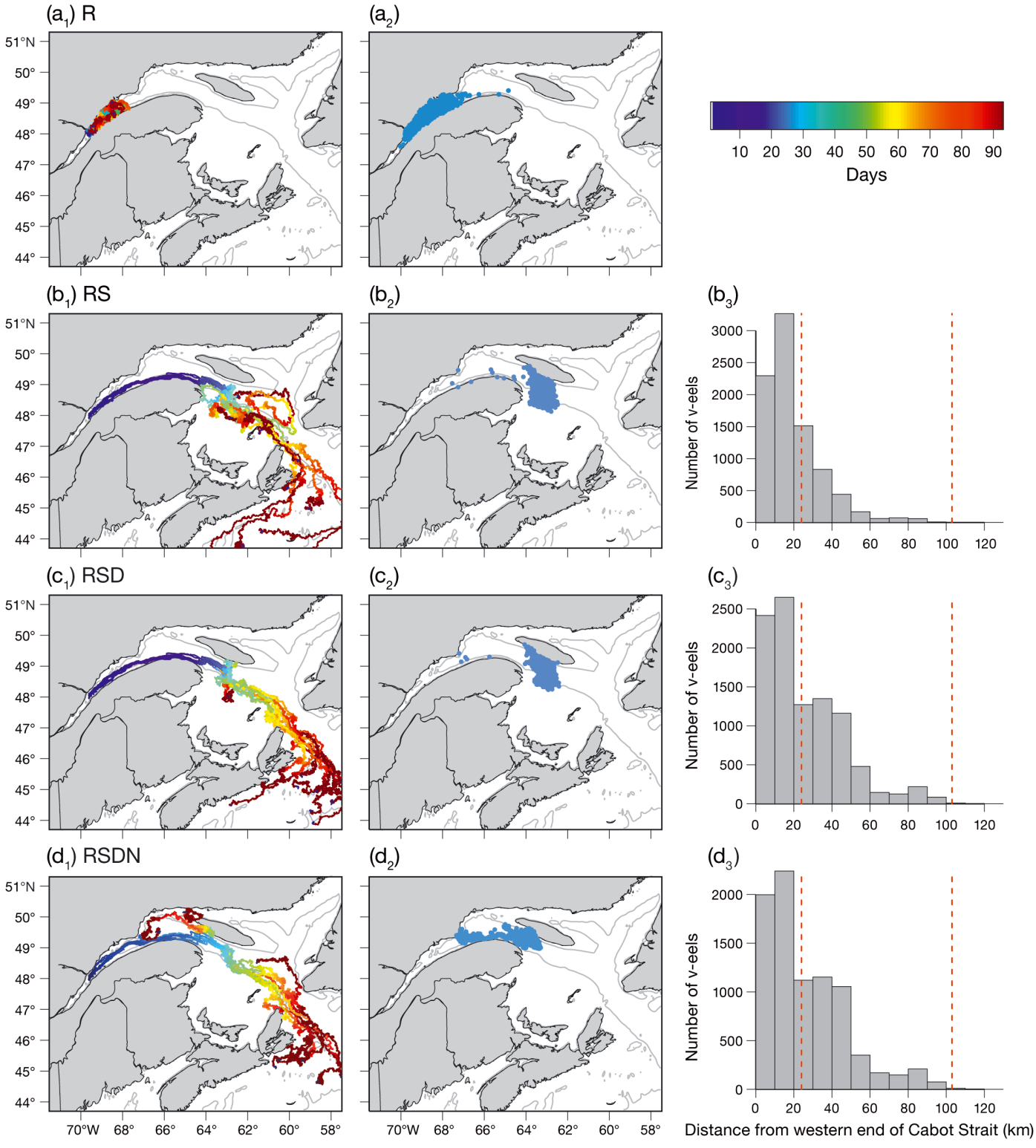

Fig. 3. Results from virtual eel (v-eel) numerical simulations (a) R, (b) RS, (c) RSD, (d) RSDN, (e) DB, (f) DBP, (g) DBW, (h) OD, (i) OS and (j) OSD (see Table 1 for simulation descriptions), showing trajectories of 10 randomly selected v-eels (left panels, subscript 1), location of all v-eels (N = 11 921) after 28 d of tracking (middle panels, subscript 2), and location of v-eels when crossing Cabot Strait (right panels, subscript 3). A color gradient is used to visualize the location of v-eels over time (each day is a different color). Red dashed lines in panels (b_3–h_3) represent location of 200 m isobaths (i.e. delineate the Laurentian Channel). Note that in simulations R, OS, and OSD, no v-eels crossed Cabot Strait during the tracking period, therefore no histogram of their distribution at that location could be drawn

(Fig. continued on next page)

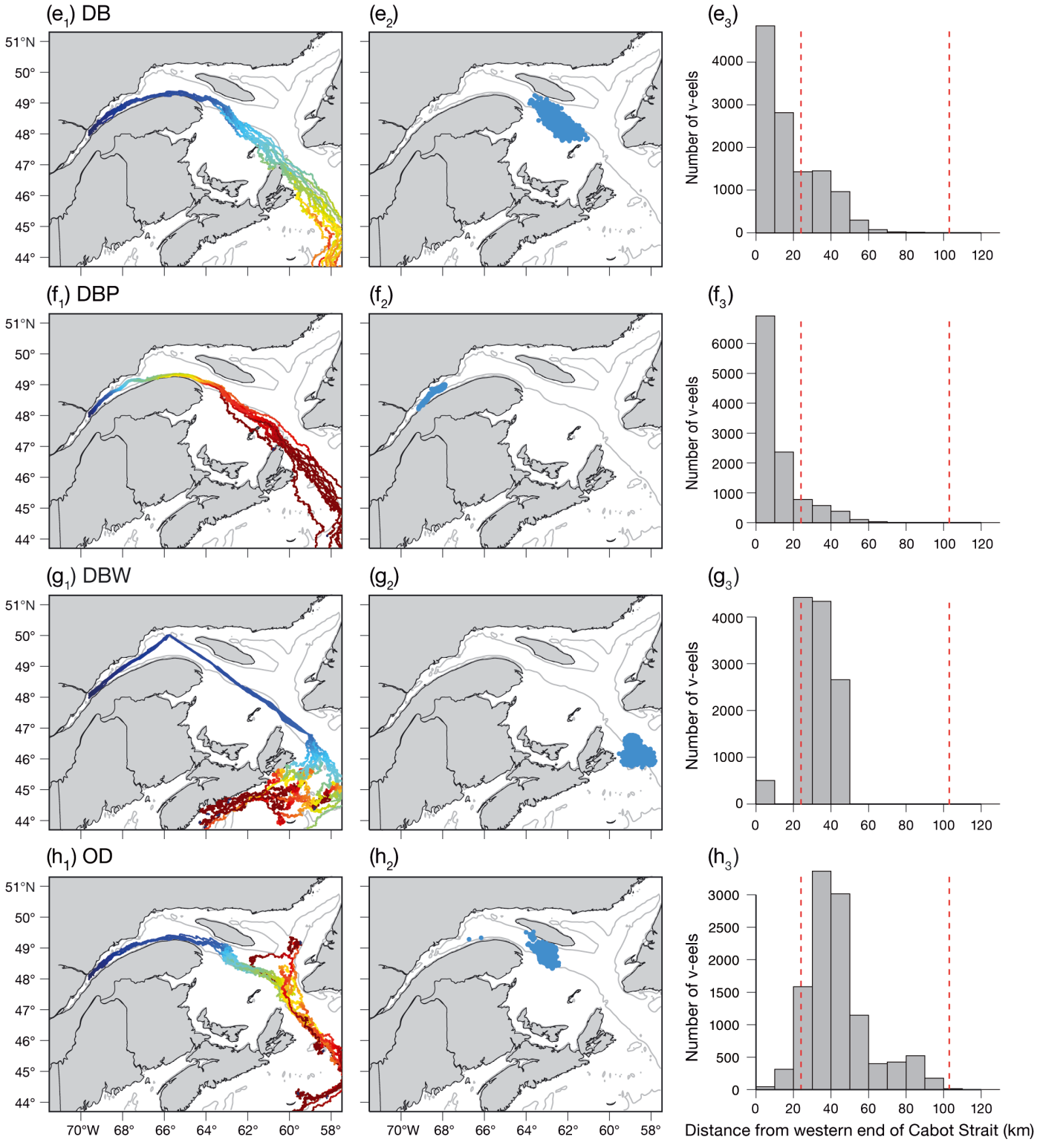

Fig. 3 (continued)

(Fig. continued on next page)

success rate (0% after 67 d of tracking), compared to the v-eels in simulation DB (ca. 10 d to reach 67.125° W, and 100% success after 67 d of tracking; Table 2, Figs. 3e$_2$,f$_2$ & 4).

Model results demonstrated that simple environmental gradients of salinity and water depths were not sufficient to explain the observed migratory performance of eels traversing the GSL. Simulations in

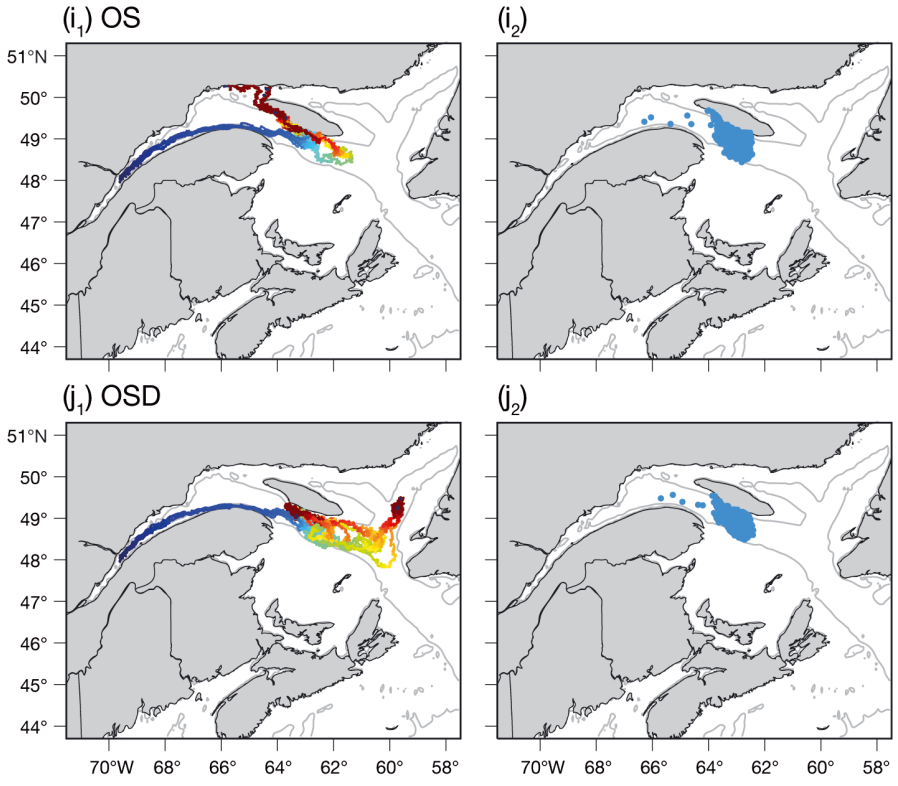

Fig. 3 (continued)

which a compass orientation toward Cabot Strait was used by v-eels were by far the most successful among all numerical simulations, with 100% of v-eels reaching the Gulf within 20 and 49 d in DBW and DB, respectively (Fig. 4). At a constant swimming speed of 0.5 m s^{-1}, none of the other numerical simulations allowed v-eels to either reach Cabot Strait within 45 d or to reach the maximal success rate (100%) before the end of the tracking period. Success in simulations R, OS, and OSD was null (no v-eels reached Cabot Strait within the tracking period; Fig. 3a,i,j), whereas OD, RSD and RS had success rates of 71.7, 49.3 and 33.5%, respectively after 67 d (Table 2, Fig. 4). In the latter 3 cases, no v-eels reached Cabot Strait within the time window observed for most tagged eels (20 to 37 d), and the success reached a plateau (ca. 77.6% of successful v-eels) soon after 67 d of tracking in OD.

Inclusion of the DVM behaviour slightly improved the success of migration. Indeed, in simulation RSD (in which DVM was implemented), 49.5% of the v-eels reached Cabot Strait 67 d after their release from the Estuary, compared to 33.5% for v-eels in RS (in which DVM was not implemented; Table 2, Fig. 4). At 28 d after release, the mean spread of the v-eels around their centre of mass in RSD was lower than in RS (16.1 ± 12.0 and 17.1 ± 12.7 km, respectively), showing a higher dispersion of v-eels when DVM was not used (Fig. $3b_2$,c_2).

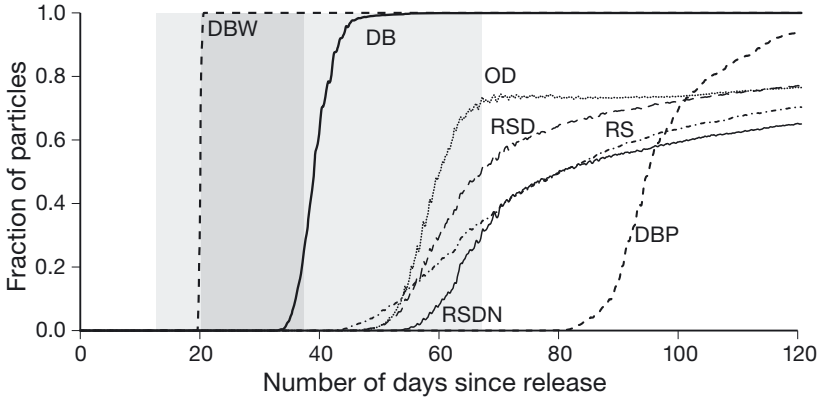

Fig. 4. Success of virtual eels (v-eels) in reaching the southern end of the Gulf of St. Lawrence at Cabot Strait with various vertical and horizontal behaviours, with a horizontal swimming speed of 0.5 m s^{-1}. V-eels were released on 28 Oct 2011 and tracked for 120 d (N = 11 921 v-eels for each simulation). Shaded rectangles: time frame of field tracking experiments conducted between 2011 and 2013 (eels tagged in the St. Lawrence Estuary and detected at Cabot Strait); darkest rectangle: when most eels were detected (20 to 37 d after release). See Table 1 for simulation abbreviations

Trajectories of v-eels and location across Cabot Strait

In all numerical simulations except for DBW and R, v-eels migrated close to the south shore of the SLR while in the lower SLE (Fig. 3). In the Gulf, v-eels in simulations OD, RS, RSD, DB and DBP migrated along the Laurentian Channel, whereas most v-eels in OSD migrated either toward the northeastern part of the Gulf or moved back to an area south of Anticosti Island (the latter also occured in simulation OS). The along-transect positions of successful v-eels as they crossed Cabot Strait varied among numerical sim-

ulations, but none of the v-eels from any simulation crossed Cabot Strait on its northern side (i.e. within 20 km of Newfoundland; Fig. 3, right panels). In simulations RS, RSD, DB, and DBP, most v-eels crossed Cabot Strait within 20 km of its southern side (i.e. in a shallower area close to St. Paul Island), whereas in OD, v-eels were in the middle of the Laurentian Channel when escaping the Gulf.

Effect of swimming speeds

Success and duration of the v-eels' migration in the Gulf relied to a large extent on individual swimming speeds (which are independent of currents in our model) but in a different way among all numerical simulations (Figs. 5 & 6). For those simulations in which success after 120 d did not reach 100%, success was at first slightly improved by greater horizontal swimming speeds but remained very low at the end of the 120 d. For example, in simulation OD, success remained <50% after 67 d of tracking regardless of swimming speed, and only ~3.3% of v-eels swimming at 1.5 m s^{-1} were able to reach Cabot Strait within 38 d (Fig. 5).

In simulation DB, where success reached 100% long before the end of the tracking period, the duration of migration increased exponentially as swimming speed decreased (Fig. 6). The various horizontal swimming speeds tested in DB allowed reproduction of the range of transit times observed in the field for acoustically tagged eels (i.e. between 13 and 68 d). Only v-eels swimming at speeds >1.0 m s^{-1} (between 1.2 and 1.5 m s^{-1}) were able to reach Cabot Strait within 20 d in DB, while swimming at half that speed (0.5 m s^{-1}) was required for v-eels in DBW. In DB, v-eels swimming between 0.6 and 1.0 m s^{-1} reached Cabot Strait within the time observed for most eels (20 to 38 d).

Effect of river discharge

Our model results demonstrated that the SLR discharge specified in the ocean circulation model significantly affected the duration of v-eels' migration in the GSL (Fig. 7). The simulation in which v-eels performed STST in the Estuary and had a preference for swimming towards the southeast at a constant swimming speed of 0.5 m s^{-1} (simulation DB) demonstrated that the total duration of migration increased by 10 d on average when the SLR discharge was low (dry year) compared with when discharge was high

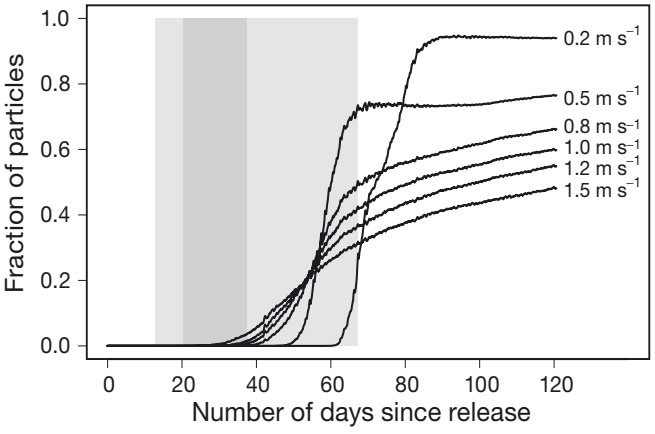

Fig. 5. Effect of horizontal swimming speeds in simulation OD (orientation toward greater depth, selective tidal stream transport [STST], and diel vertical migration [DVM]; see Table 1) on success of virtual eels (v-eels) in reaching the southern end of the Gulf at Cabot Strait. Grey rectangles: time frame of field tracking experiments conducted between 2011 and 2013 (eels tagged in the St. Lawrence Estuary and detected at Cabot Strait); darkest rectangle: when most eels were detected (20 to 37 d after release)

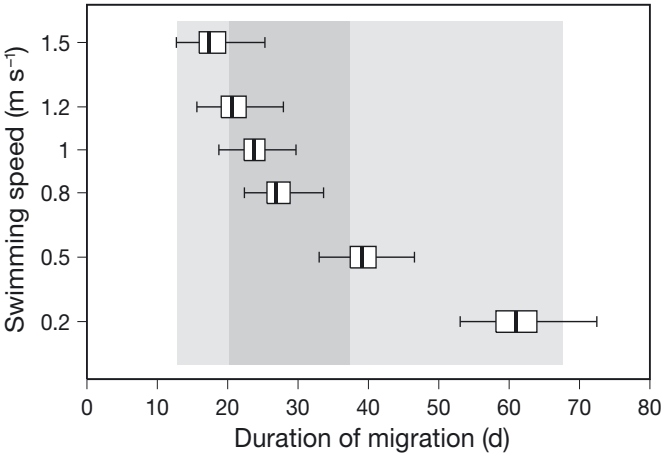

Fig. 6. Effect of horizontal swimming speed (constant swimming) on duration of virtual eel (v-eel) migration between the St. Lawrence Estuary (SLE) and Cabot Strait in simulation DB (in which v-eels are performing selective tidal stream transport [STST] while in the Estuary, diel vertical migration [DVM] in the Gulf, and swim with a preference for the southeast after exiting the SLE; see Table 1). Grey rectangles: time frame of field tracking experiments conducted between 2011 and 2013 (eels tagged in the SLE and detected at Cabot Strait); darkest rectangle: when most eels were detected (20 to 37 d after release). The vertical lines on the left and on the right of each boxplot define the minimum and maximum duration of migration, respectively. The median duration is represented by the heavy line inside each box. The left and right limits of the box define the lower and upper quartile, respectively

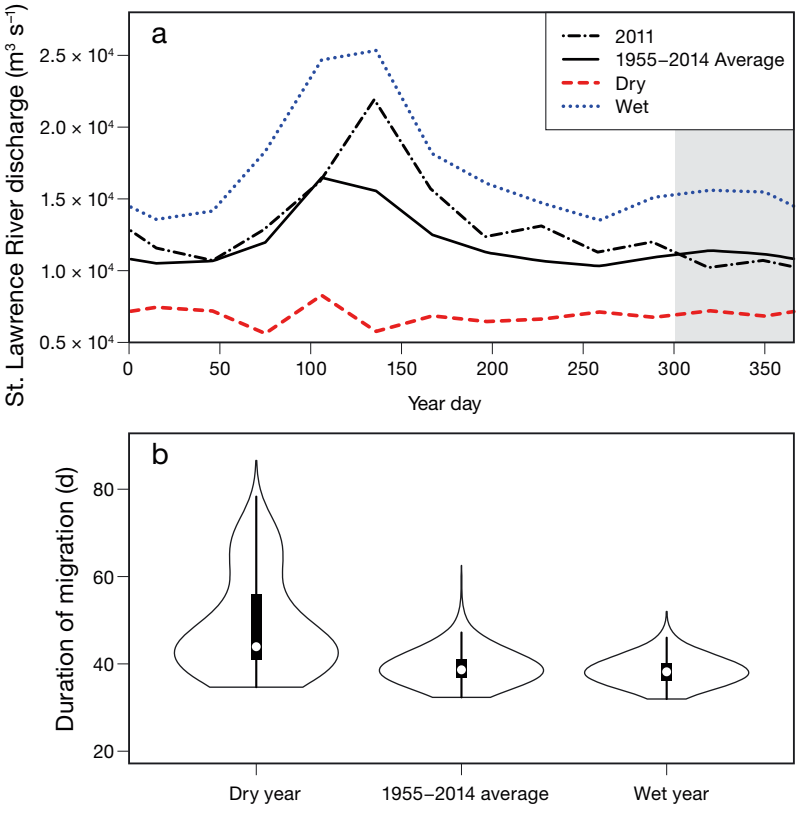

Fig. 7. (a) Daily values of St. Lawrence River (SLR) discharge interpolated from monthly-mean values at Québec City for 2011 (dashed-dotted black line), using the 1955–2014 mean (solid black line), for a wet year (blue dotted line) and for a dry year (red dashed line). See text for definitions of wet and dry years. River discharge data were downloaded from the St. Lawrence Global Observatory website: http://slgo.ca/en/runoffs/data/tables.html. Shaded rectangle: period during which silver American eels migrate from the St. Lawrence Estuary to the Gulf. (b) Effect of SLR discharge on the duration of virtual eel (v-eel) migration in simulation DB (swimming speed of 0.5 m s^{-1}; see Table 1). The shape of the violins shows the distributional characteristics of the data. Each violin is composed of a box plot and a kernel density plot. The median duration of migration is represented by the white circle inside each black box. The bottom and top limits of each black box define the lower and upper quartile, respectively. On each side of the boxplot, a kernel density estimation (distribution of duration migration frequency) is overlaid

(wet year). Whereas 99% of the v-eels migrating under the high river discharge condition reached Cabot Strait within 46 d, only ~39.4% of v-eels migrating under the low river discharge condition reached Cabot Strait within that time (v-eels in this simulation took up to 82 d to reach Cabot Strait). The difference in migration duration between an average year and wet year was significant (t = −18.7, df = 22862, $p < 0.001$) but small: 0.7 d on average. It should be noted that the SLR discharge in 2011 (the year used for this study) was very similar to the average value over the 1955 to 2014 period.

DISCUSSION

Numerical simulations conducted in this study provide evidence that American eels migrating through the SLE–GSL system must use behavioural strategies, including active swimming and highly directed orientation, in order to complete this portion of their migration within the time frame observed by acoustic tracking of eels in the field. The most successful numerical simulation of v-eel migration in the GSL required either (1) navigation to the SLE exit and then to Cabot Strait or (2) the use of STST in the SLE combined with a preference for southeastward swimming after exiting the SLE. Nevertheless, the use of tidal currents in the appropriate current direction (STST) was sufficient to allow v-eels to escape entrapment caused by the estuarine circulation in the SLE. Our simulations also demonstrated that eels performing STST must actively swim rather than drift with the seaward tidal currents to escape the Estuary within 2 wk, and then to exit the GSL through Cabot Strait within the time observed in the field (2 mo). STST is both a transport mechanism and a means of orienting and moving in an appropriate direction (Forward & Tankersley 2001, Gibson 2003). The entrainment cues for STST remain poorly understood, although olfactory cues seem to be the most likely candidate among a number of other possible environmental cues such as variations in pressure, salinity, temperature, and electric field strength (Creutzberg 1959, Forward & Tankersley 2001). The use of STST during early life-history stages has been reported in eels (e.g. Creutzberg 1959, McCleave & Kleckner 1982) but this behaviour appears equivocal, and has never been clearly demonstrated for the silver eel stage (Parker & McCleave 1997, Bradford et al. 2009). In the SLE, recent acoustic tracking simulations strongly suggest that silver eels use nocturnal ebb-tide transport (Béguer-Pon et al. 2014), although the absence of information on eel depths prevented the authors from categorically concluding that eels did

use STST. In their study, it was not known whether eels were actively swimming or drifting while migrating down the freshwater and brackish sections of the SLE. Our numerical simulations indicated that STST is likely used by eels in the SLE, assuming they actively swim with appropriate outgoing ebb tidal currents. Whether v-eels swam only at night or during both night and day while performing STST in the Estuary significantly affected the success and total duration of migration in our model. Eels moving only at night can logically escape the GLS later than eels moving 24 h a day; however both behaviours allowed v-eels to escape the SLE within 2 wk.

Our numerical simulations also suggested that it is very unlikely that eels use the horizontal salinity gradient, either alone or in combination with the water depth gradient, to orientate in the Gulf toward Cabot Strait. Most v-eels that used salinity to orient themselves moved back to the western part of the GSL once they reached the southern tip of Anticosti Island. V-eels that had a preference for both higher salinity and greater water depths migrated toward the northeastern end of the GSL. Results of previous numerical simulations (Ohashi & Sheng 2015) demonstrated that the frequency with which v-eels checked their surroundings to orientate themselves affected the model results. The more often v-eels checked their surroundings, the less successful was their migration, indicating that a strategy to detect large-scale gradients and ignore small-scale changes must be used by out-migrating animals. How eels or any other species evaluate salinity at large spatial scales is unknown. Orientation toward greater water depth lead to some success in the model, with a high probability (72%) of reaching Cabot Strait after 67 d of migration, but no v-eels using that orientation behaviour were able to reach Cabot Strait within 1 mo. Thus, this behaviour alone cannot explain the duration of migration observed by telemetry experiments. The limited success can be partly explained by the bathymetry of the GSL, in which water depth does not increase monotonically from the SLE towards Cabot Strait but rather is characterized by the multi-branched Laurentian Channel. The ability of eels (and fish in general) to measure depth has long been assumed unlikely. However, recent studies have demonstrated that fish are able to sense changes in ambient pressure through changes in their swim bladder volume, and can combine this information with their vertical speed to determine their vertical location (Taylor et al. 2010, Holbrook & de Perera 2011). Satellite tagging experiments conducted on silver eels in the GSL (Béguer-Pon et al. 2012), coupled with detections of acoustically tagged eels (authors' unpubl. data) suggest that eels migrate along the main branch of the Laurentian Channel while in the Gulf. Trajectories of v-eels in our numerical simulations showed that an orientation mechanism based on depth allowed reproduction of the suggested migratory path in the GSL and the observed distribution of acoustic detections at Cabot Strait (concentrated on the western part of the Laurentian Channel and Cabot Strait). We therefore cannot exclude the water depth cue as an orientation mechanism; however, other cues must be involved in order to reproduce the observed success of migration.

Comparison between simulations in which v-eels used and did not use DVM (RS and RSD, respectively) showed that the use of DVM slightly decreased the dispersion of v-eels. V-eels performing DVM were programmed to change their depth twice a day, all at the same depth — thus they experienced similar circulation fields assuming the horizontal variation in currents at a given depth was not very large. On the contrary, v-eels that did not perform DVM were free to move vertically (due to both vertical currents and very small random vertical movements that mimicked small-scale mixing) and thus experienced various currents, leading to a higher dispersion. The DVM behaviour has been observed in several anguillid species migrating in the ocean, and it has been hypothesized that this behaviour may be a trade-off between predator avoidance and thermoregulation (e.g. Aarestrup et al. 2009, Schabetsberger et al. 2013). If field observations were to show that eels leaving the continent occupy the same depth layers on a daily basis during their oceanic migration, such observations would strengthen our suggestion that DVM also plays a significant role in limiting the dispersion of eels during their migration.

Our most successful numerical simulations involved either navigation toward the SLE exit and then toward Cabot Strait, or a preference for southeastward swimming after exiting the SLE with the help of STST. Although these results appear quite logical (v-eels being programmed to swim in the correct directions), these scenarios allow for an assessment of the duration of migration and an evaluation of the realism of such behaviours. In simulation DB, where v-eels used STST to escape the Estuary and then swam with a preference for the southeast, a swimming speed between 0.5 and 1.0 m s^{-1} was required to reach Cabot Strait within 20 to 38 d (the time observed for most eels acoustically tracked in the GSL). For 1 m long eels, these values are close to the optimal swimming speeds evaluated in labora-

tory experiments (0.7 and 1.0 BL s^{-1}; e.g. van den Thillart & van Ginneken 2007, Burgerhout et al. 2013a), reinforcing our confidence that DB is realistic. In the most successful simulation, DBW, in which v-eels swam constantly toward the SLE exit and then toward Cabot Strait, swimming speeds <0.5 m s^{-1} allowed v-eels to reach Cabot Strait within 20 d, indicating that if eels used that behaviour at sea, they would be swimming at between 0.1 and 0.6 m s^{-1}. However, this behaviour would require more energy expenditure than the one that includes STST in the Estuary, since actively swimming only when the current is in the appropriate direction allows significant energy savings (Weihs 1978). The use of STST could also possibly be advantageous in terms of immediate survival by minimizing the time spent in the water column, and thus reducing the risk of predation mortality (McCleave & Wippelhauser 1987), especially if STST only occurs at night (Béguer-Pon et al. 2014).

The mechanism for such orientation/navigation behaviours could be based on a complex combination of environmental factors acting together (salinity, odour, water depth, temperature) and/or could rely on the ability of eels to sense and use the geomagnetic field. Durif et al. (2013) recently showed that eels can sense the geomagnetic field and can orientate themselves toward a direction previously imprinted. The geomagnetic field intensity decreases from the northwestern to the southeastern part of the Gulf; it could thus act as cue for orientation toward the southeast. We do not know what mechanisms could enable a switch from an estuarine STST behaviour to a southeast swimming direction in simulations DB and DBW, but an inherited or imprinted bi-dimensional map based on a combination of geomagnetic intensity and inclination angle could be involved, as proposed for Pacific salmon (Putman et al. 2014). Eels could have true navigation abilities, as suggested by recent satellite tagging experiments conducted in the open ocean on American eels (Béguer-Pon et al. 2015).

Low detection rates of acoustic tags by receiver arrays is a common problem in telemetry studies and may be related to either loss of fish due to mortality or poor receiver performance such that the fish are present but not recorded (Heupel et al. 2006). Results from our numerical simulations could be used to evaluate the hypothesis that the low detection rate is due to low detection efficiency, and help guide future telemetry array design. Results from all our numerical simulations show that no v-eels crossed Cabot Strait at its eastern part. This result may be explained by the presence of currents entering the GSL through northeastern Cabot Strait, which create unfavourable conditions for leaving the GSL. This suggests that low detection rate at the northeastern part of Cabot Strait is likely due to an actual absence of tagged animals rather than low detection efficiency. Because acoustic receivers across Cabot Strait are only deployed close to the bottom (max. water depth: 480 m), additional receivers should be deployed closer to the surface, especially in the southwestern part of the Strait, in order to increase the probability of detecting migrating eels.

The model presented here could also be used as a tool for evaluating the potential effect of climate change on the timing of eels' migration out of the GSL. The numerical simulations conducted using various extreme SLR discharge conditions showed that the duration of v-eels' migration in the Gulf increased by an average of 10 d during low discharge compared to high discharge years. The effect of freshwater discharge on the seaward migration of silver eels has been widely documented in rivers and fluvial estuaries (e.g. Vøllestad et al. 1986, de Lafontaine et al. 2009, Verreault et al. 2012). The hydrological regime of the SLR and its tributaries is projected to be affected by climate change (Boyer et al. 2010). The numerical simulations conducted in our study represent a first step in exploring the effect of SLR discharge on the timing of migration out of the Gulf; more simulations that include the discharge of tributaries and their projected changes from various scenarios of climatic change are needed in order to address this important question.

Acknowledgements. Funding for this project was provided to J.J.D., M.C., and J.S. by the Ocean Tracking Network through a strategic network grant (NETGP #375118-08) from the Canadian Natural Sciences and Engineering Research Council of Canada (NSERC) with additional funding from the Canadian Foundation for Innovation (CFI, Project #13011).

LITERATURE CITED

Aarestrup K, Økland F, Hansen MM, Righton D and others (2009) Oceanic spawning migration of the European eel (*Anguilla anguilla*). Science 325:1660

Bauer S, Klaassen M (2013) Mechanistic models of animal migration behaviour – their diversity, structure and use. J Anim Ecol 82:498–508

Béguer-Pon M, Benchetrit J, Castonguay M, Aarestrup K, Campana SE, Stokesbury MJW, Dodson JJ (2012) Shark predation on migrating adult American eels (*Anguilla rostrata*) in the Gulf of St. Lawrence. PLoS ONE 7:e46830

Béguer-Pon M, Castonguay M, Benchetrit J, Hatin D and others (2014) Large-scale migration patterns of silver American eels from the St. Lawrence River to the Gulf

using acoustic telemetry. Can J Fish Aquat Sci 71: 1579–1592

Béguer-Pon M, Castonguay M, Shan S, Benchetrit J, Dodson JJ (2015) Direct observations of American eels migrating across the continental shelf to the Sargasso Sea. Nat Commun 6:8705

Béguer-Pon M, Shan S, Thompson K, Castonguay M, Sheng J, Dodson JJ (2016) Exploring the role of the physical marine environment on silver eel migration using a biophysical particle-tracking model. ICES J Mar Sci 73:57–74

Bonhommeau S, Blanke B, Tréguier AM, Grima N and others (2009) How fast can the European eel (*Anguilla anguilla*) larvae cross the Atlantic Ocean? Fish Oceanogr 18:371–385

Bourgault D, Koutitonsky VG (1999) Real-time monitoring of the freshwater discharge at the head of the St. Lawrence Estuary. Atmos-Ocean 37:203–220

Boyer C, Chaumont D, Chartier I, Roy AG (2010) Impact of climate change on the hydrology of St. Lawrence tributaries. J Hydrol (Amst) 384:65–83

Bradford RG, Carr JW, Page FH, Whoriskey F (2009) Migration of silver American eels through a macrotidal estuary and bay. Am Fish Soc Symp 69:275–292

Burgerhout E, Brittijn SA, Tudorache C, de Wijze DL, Dirks RP, van den Thillart GEEJM (2013a) Male European eels are highly efficient long distance swimmers: effects of endurance swimming on maturation. Comp Biochem Physiol A Mol Integr Physiol 166:522–527

Burgerhout E, Tudorache C, Brittijn SA, Palstra AP, Dirks RP, van den Thillart GEEJM (2013b) Schooling reduces energy consumption in swimming male European eels, *Anguilla anguilla* L. J Exp Mar Biol Ecol 448:66–71

Castonguay M, Hodson PV, Couillard CM, Eckersley MJ, Dutil JD, Verreault G (1994) Why is recruitment of the American eel, *Anguilla rostrata*, declining in the St. Lawrence River and Gulf? Can J Fish Aquat Sci 51: 479–488

Castonguay M, Comeau L, Swain D, Bowen D, O'Dor R, Stokesbury M, Branton R (2015) OTN Cabot Strait Line – metadata and data set. In: O'Dor R, Whoriskey F, Branton R, Gross T (eds) Ocean tracking network global equipment deployments and data collection. http://members.oceantrack.org/data/discovery/CBS.htm (accessed 18 June 2015)

Chow S, Okazaki M, Watanabe T, Segawa K and others (2015) Light-sensitive vertical migration of the Japanese eel *Anguilla japonica* revealed by real-time tracking and its utilization for geolocation. PLoS ONE 10:e0121801

COSEWIC (2012) COSEWIC assessment and status report on the American eel *Anguilla rostrata* in Canada. Committee on the Status of Endangered Wildlife in Canada, Ottawa

Côté CL, Gagnaire PA, Bourret V, Verreault G, Castonguay M, Bernatchez L (2013) Population genetics of the American eel (*Anguilla rostrata*): F_{ST} = 0 and North Atlantic Oscillation effects on demographic fluctuations of a panmictic species. Mol Ecol 22:1763–1776

Creutzberg F (1959) Discrimination between ebb and flood tide in migrating elvers (*Anguilla vulgaris* Turt.) by means of olfactory perception. Nature 184:1961–1962

de Lafontaine Y, Lagacé M, Gingras F, Labonté D, Marchand F, Lacroix E (2009) The decline of the American eel in the St. Lawrence River: effects of local hydroclimatic conditions on CPUE indices. Am Fish Soc Symp 58: 207–229

Durif CMF, Browman HI, Phillips JB, Skiftesvik AB, Vøllestad LA, Stockhausen HH (2013) Magnetic compass orientation in the European eel. PLoS ONE 8:e59212

Egbert GD, Erofeeva SY (2002) Efficient inverse modeling of barotropic ocean tides. J Atmos Ocean Technol 19: 183–204

Forward RB, Tankersley RA (2001) Selective tidal-stream transport of marine animals. Oceanogr Mar Biol Annu Rev 39:305–353

Geshelin Y, Sheng J, Greatbatch RJ (1999) Monthly mean climatologies of temperature and salinity in the western North Atlantic. Can Tech Rep Hydrogr Ocean Sci 153: 1–62

Gibson RN (2003) Go with the flow: tidal migration in marine animals. Hydrobiologia 503:153–161

Healey MC, Thomson KA, Leblond PH, Huato L, Hinch SG, Walters CJ (2000) Computer simulations of the effects of the Sitka eddy on the migration of sockeye salmon returning to British Columbia. Fish Oceanogr 9: 271–281

Heupel MR, Semmens JM, Hobday AJ (2006) Automated acoustic tracking of aquatic animals: scales, design and deployment of listening station arrays. Mar Freshw Res 57:1–13

Holbrook RI, de Perera TB (2011) Fish navigation in the vertical dimension: Can fish use hydrostatic pressure to determine depth? Fish Fish 12:370–379

Hussey NE, Kessel ST, Aarestrup K, Cooke SJ and others (2015) Aquatic animal telemetry: a panoramic window into the underwater world. Science 348:1255642

Jessop BM (2010) Geographic effects on American eel (*Anguilla rostrata*) life history characteristics and strategies. Can J Fish Aquat Sci 67:326–346

Ji X, Sheng J, Tang L, Liu D, Yang X (2011) Process study of circulation in the Pearl River Estuary and adjacent coastal waters in the wet season using a triply-nested circulation model. Ocean Model 38:138–160

Kettle AJ, Haines K (2006) How does the European eel (*Anguilla anguilla*) retain its population structure during its larval migration across the North Atlantic Ocean? Can J Fish Aquat Sci 63:90–106

Koutitonsky VG, Bugden GL (1991) The physical oceanography of the Gulf of St. Lawrence: a review with emphasis on the synoptic variability of the motion. In: Therriault JC (ed) The Gulf of St. Lawrence: Small ocean or big estuary? Can Spec Publ Fish Aquat Sci 113:57–90

McCleave JD, Kleckner RC (1982) Selective tidal stream transport in the estuarine migration of glass eels of the American eel (*Anguilla rostrata*). J Cons Int Explor Mer 40:262–271

McCleave JD, Wippelhauser GS (1987) Behavioural aspects of selective tidal stream transport in juvenile American eels. Am Fish Soc Symp 1:138–150

Mellor G (2004) Users guide for a three-dimensional, primitive equation, numerical ocean circulation model. Princeton University, Princeton, NJ

Mesinger F, DiMego G, Kalnay E, Mitchell K and others (2006) North American regional reanalysis. Bull Am Meteorol Soc 87:343–360

Ohashi K, Sheng J (2013) Influence of St. Lawrence River discharge on the circulation and hydrography in Canadian Atlantic waters. Cont Shelf Res 58:32–49

Ohashi K, Sheng J (2015) Investigating the effect of the physical environment and swimming behaviours on the movement of particles in the Gulf of St. Lawrence using

an individual-based numerical model. Atmos-Ocean, doi:10.1080/07055900.2015.1090390
Parker SJ, McCleave JD (1997) Selective tidal stream transport by American eels during homing movements and estuarine migration. J Mar Biol Assoc UK 77:871–889
Putman NF (2015) Inherited magnetic maps in salmon and the role of geomagnetic change. Integr Comp Biol 55:396–405
Putman NF, Scanlan MM, Billman EJO, Neil JP and others (2014) An inherited magnetic map guides ocean navigation in juvenile Pacific salmon. Curr Biol 24:446–450
Rypina I, Llopiz JK, Pratt LJ, Lozier MS (2014) Dispersal pathways of American eel larvae from the Sargasso Sea. Limnol Oceanogr 59:1704–1714
Schabetsberger R, ØKland F, Aarestrup K, Kalfatak D and others (2013) Oceanic migration behaviour of tropical Pacific eels from Vanuatu. Mar Ecol Prog Ser 475:177–190
Tang W, Bennett DA (2010) Agent-based modeling of animal movement: a review. Geogr Compass 4:682–700
Taylor GK, Holbrook RI, de Perera TB (2010) Fractional rate of change of swim-bladder volume is reliably related to absolute depth during vertical displacements in teleost fish. J R Soc Interface 7:1379–1382
Thomson KA, Ingraham WJ, Healey MC, Leblond PH, Groot C, Healey CG (1992) The influence of ocean currents on latitude of landfall and migration speed of sockeye salmon returning to the Fraser River. Fish Oceanogr 1:163–179
Thomson KA, Ingraham WJ, Healey MC, Leblond PH, Groot C, Healey CG (1994) Computer simulations of the influence of ocean currents on Fraser River sockeye salmon (*Oncorhynchus nerka*) return times. Can J Fish Aquat Sci 51:441–449
Tremblay V (2009) Reproductive strategy of female American eels among five subpopulations in the St. Lawrence River watershed. Am Fish Soc Symp 58:85–102
Urrego-Blanco J, Sheng J (2012) Interannual variability of the circulation over the eastern Canadian shelf. Atmos-Ocean 50:277–300
van den Thillart G, Palastra A, van Ginneken V (2007) Simulated migration of European silver eel; swim capacity and cost of transport. J Mar Sci Technol Spec Issue:1–16
Verreault G, Mingelbier M, Dumont P (2012) Spawning migration of American eel *Anguilla rostrata* from pristine (1843–1872) to contemporary (1963–1990) periods in the St. Lawrence Estuary, Canada. J Fish Biol 81:387–407
Vøllestad LA, Jonsson B, Hvidsten NA, Næsje TF, Haraldstad Ø, Ruud-Hansen J (1986) Environmental factors regulating the seaward migration of European silver eels (*Anguilla anguilla*). Can J Fish Aquat Sci 43:1909–1916
Weihs D (1978) Tidal stream transport as an efficient method for migration. J Cons Int Explor Mer 38:92–99
Wysujack K, Westerberg H, Aarestrup K, Trautner J, Kurwie T, Nagel F, Hanel R (2015) The migration behaviour of European silver eels (*Anguilla anguilla*) released in open ocean conditions. Mar Freshw Res 66:145–157

Appendix. Description of the ocean circulation model

The numerical ocean circulation model whose output was used in the individual-based model is briefly described here. Please refer to Ohashi & Sheng (2013, 2015) for more detailed descriptions and discussions of comparisons between the fields simulated by this model and their observed counterparts.

The model bathymetry is based on the 30-arcsecond resolution General Bathymetric Chart of the Oceans (www.gebco.net), and has a minimum water depth of 10 m and a maximum water depth of about 5780 m. At the sea surface, the model is driven by 3-hourly atmospheric forcing derived from the North American Regional Reanalysis dataset (Mesinger et al. 2006). Along its lateral open boundaries, the model is driven by 3 types of fields: (1) hourly values of sea level and depth-averaged currents produced by a barotropic version of the model that covers the eastern Canadian seaboard; (2) hourly values of tidal sea level and depth-averaged currents, derived from the 'East coast of the USA' dataset of Oregon State University Tidal Prediction Software (Egbert & Erofeeva 2002); and (3) daily climatological values of 3D temperature, salinity, and currents derived from a 17 yr (1988 to 2004) simulation made with an ocean circulation model covering the northwest Atlantic (Urrego-Blanco & Sheng 2012). Rivers are represented in an idealized manner by channels cut into the model's coastline (Fig. 1). Daily values of river discharge are specified at the heads of the rivers using the method described by Ji et al. (2011). For the SLR, daily discharge values were derived by temporal interpolation from monthly discharge estimates for the study period made by the Canadian Hydrographic Service using the method described by Bourgault & Koutitonsky (1999), available on the St. Lawrence Global Observatory website (http://slgo.ca/en/runoffs/data/tables.html). For all other rivers, daily discharge values were obtained by temporal interpolation of monthly climatological discharge values, calculated from observations made by the Water Survey of Canada (http://wateroffice.ec.gc.ca/).

Calibration and validation of the circulation model was made previously by comparing model results with observations for tidal elevations, currents, and hydrography (Ohashi & Sheng (2013, 2015). Agreement between observed and simulated values ranged from 'very good' for tidal elevations to 'reasonable' for currents (which are more difficult to simulate accurately). In this study, the ocean circulation model was initialized with monthly-mean climatological fields of temperature and salinity (authors' unpubl. data processed using the methodology of Geshelin et al. 1999). The circulation model was integrated for 26 mo beginning 1 January 2010.

Editorial responsibility: Alejandro Gallego, Aberdeen, UK

Submitted: November 17, 2015; Accepted: March 22, 2016
Proofs received from author(s): April 21, 2016